E-Article

Synchrony and Perturbation Transmission in Trophic Metacommunities

Pierre Quévreux,* Matthieu Barbier, and Michel Loreau

Theoretical and Experimental Ecology Station, CNRS Unité Mixte de Recherche (UMR) 5321, 09200 Moulis, France

Submitted March 31, 2020; Accepted November 24, 2020; Electronically published April 19, 2021

Online enhancements: supplemental PDF.

abstract: In a world where natural habitats are ever more fragmented, the dynamics of metacommunities are essential to properly understand species responses to perturbations. If species' populations fluctuate asynchronously, the risk of their simultaneous extinction is low, thus reducing the species' regional extinction risk. However, identifying synchronizing or desynchronizing mechanisms in systems containing several species and when perturbations affect multiple species is challenging. We propose a metacommunity model consisting of two food chains connected by dispersal to study the transmission of small perturbations affecting populations in the vicinity of an equilibrium. In spite of the complex responses produced by such a system, two elements enable us to understand the key processes that rule the synchrony between populations: (1) knowing which species have the strongest response to perturbations and (2) the relative importance of dispersal processes compared with local dynamics for each species. We show that perturbing a species in one patch can lead to asynchrony between patches if the perturbed species is not the most affected by dispersal. The synchrony patterns of rare species are the most sensitive to the relative strength of dispersal to demographic processes, thus making biomass distribution critical to understanding the response of trophic metacommunities to perturbations. We further partition the effect of each perturbation on species synchrony when perturbations affect multiple trophic levels. Our approach allows disentangling and predicting the responses of simple trophic metacommunities to perturbations, thus providing a theoretical foundation for future studies considering more complex spatial ecological systems.

Keywords: food chain, top-down, bottom-up, dispersal, coupling, biomass distribution.

Introduction

Biodiversity is under increasing anthropic perturbations that alter populations and community dynamics (e.g., the latest Intergovernmental Science-Policy Platform on Biodiversity and Ecosystem Services [IPBES] assessment; Díaz et al. 2019). In particular, species live in more and more fragmented habitats (Haddad et al. 2015), which reduce dispersal and partially isolate communities from one another. The metacommunity framework is key to addressing the responses of species and communities to perturbations in this changing world (Leibold et al. 2004; Amarasekare 2008; Leibold and Chase 2017). Small isolated populations are more prone to extinction (Purvis et al. 2000), and simultaneous local extinctions across sites lead to a global extinction. The asynchrony between different populations of the same species is a fundamental mechanism ensuring the global persistence and temporal stability of an entire metapopulation at the landscape scale, as it reduces the risk of simultaneous extinction in all patches (Blasius et al. 1999).

While dispersal tends to synchronize populations of the same species (Abbott 2011), dispersal of specific trophic levels can lead to synchrony or asynchrony between the various species in food chains (Koelle and Vandermeer 2005; Pedersen et al. 2016). Species that disperse or forage across several communities can propagate trophic cascades in space, as shown empirically and theoretically (Knight et al. 2005; McCoy et al. 2009; Casini et al. 2012; García-Callejas et al. 2019); depending on which trophic levels disperse, the strength of trophic cascades within each community can be amplified or dampened (Leroux and Loreau 2008). In addition, different food chain lengths in different sites can lead to opposite responses of different populations of the same species (Wollrab et al. 2012).

The dispersal of top predators has been particularly studied, as generalist consumers linking different food webs by feeding on multiple energetic channels are ubiquitous across ecosystems (Rooney et al. 2006, 2008; Wolkovich et al. 2014; Ward et al. 2015). In particular, mobile predatory fish couple pelagic and benthic compartments in aquatic ecosystems (Vander Zanden and Vadeboncoeur

* Corresponding author; email: pierre.quevreux@cri-paris.org.

ORCIDs: Quévreux, https://orcid.org/0000-0002-3531-1410; Barbier, https://orcid.org/0000-0002-0669-8927.

Am. Nat. 2021. Vol. 197, pp. E188–E203.
DOI: 10.1086/714131

2002; Vadeboncoeur et al. 2005), and predator dispersal leads to trophic cascades in surrounding ecosystems (Knight et al. 2005; Casini et al. 2012; Tscharntke et al. 2012). In such systems, asynchrony is promoted by the asymmetry between coupled food chains (McCann et al. 1998; Rooney et al. 2006) even when top predator populations are under correlated environmental perturbations (Vasseur and Fox 2007).

Many of these theoretical studies have considered the synchrony of food chains that display chaotic dynamics or limit cycles (McCann et al. 1998; Koelle and Vandermeer 2005; Rooney et al. 2006), which are characteristic of strong top-down control (Barbier and Loreau 2019). In this case, many of the mechanisms cited above (e.g., top predator coupling or asymmetry) act simultaneously and interact with the variability generated internally by the limit cycles of food chain dynamics, which makes it difficult to tease apart the effects of internal and external sources of variability. Variability can also be generated by stochastic external perturbations, but few studies investigating synchrony in metacommunities have considered these (McCann et al. 2005; Vasseur and Fox 2007). Wang et al. (2015) used them successfully to investigate the stability of competitive metacommunities, but their effects in trophic metacommunities remain poorly understood. In the context of stochastic perturbations, mechanisms such as asymmetry may not be required to get asynchrony between the different populations.

Here, we propose a first step toward a more systematic approach to synchrony in trophic metacommunities near equilibrium, where several species can disperse and several stochastic perturbations can affect different species independently. We aim to understand what shapes synchrony in a broad spectrum of ecological settings, dominated by either bottom-up or top-down control within a food chain (Barbier and Loreau 2019) and by either trophic or spatial mechanisms at each trophic level. To achieve this goal, it is primordial to describe the relative contribution of perturbations and dispersal compared with the local demographic dynamics among species. In a single food chain, Barbier and Loreau (2019) showed that a few parameters control the biomass distribution among trophic levels (i.e., top- or bottom-heavy pyramids) and the overall top-down or bottom-up behavior of the system (e.g., trophic cascades). In turn, the biomass distribution drives many processes in food web dynamics. For instance, Arnoldi et al. (2019) showed that the variance generated by stochastic perturbations depends on species' biomass. Thus, perturbations with the same variance can impact the dynamics of different species more or less depending on their relative abundances.

As noted above, food web dynamics can be highly sensitive to varying dispersal rates of particular trophic levels (Koelle and Vandermeer 2005; Pedersen et al. 2016). Comparing the absolute values of dispersal rates, however, is not meaningful when considering species with different biological rates Therefore, we rescale the dispersal rate of each species by its density-dependent mortality rate, which is assumed to be representative of various intraspecific processes, as done by Barbier and Loreau (2019) for all biological rates. More generally, quantifying the relative importance of local dynamics and dispersal processes is key to properly assessing how dispersal affects the overall dynamics of each species. In fact, the relative importance of local dynamics and dispersal is what distinguishes different metacommunity paradigms (Leibold et al. 2004; Leibold and Chase 2017); it also controls different recovery regimes after perturbations. For instance, Zelnik et al. (2019) showed that with low dispersal and fast local dynamics the system recovers locally from the perturbation, while with high dispersal and slow local dynamics perturbations propagate across the whole system. In our system, we can expect the biomass distribution to affect the relative importance of local dynamics and dispersal processes, as they do not scale in the same way with species biomass.

Taken together, these mechanisms must lead to situations where perturbations do not have the strongest impact on the species whose dynamics are the most impacted by dispersal. In such a situation, those perturbations can filter through the food web before being transmitted through dispersal and then affect different locations in opposite ways. A synthetic understanding of synchrony may thus be achieved by quantifying the propagation of perturbations, both vertically along food chains and horizontally across space.

We develop a model of coupled food chains based on these recent studies and first consider a perturbation affecting a unique species in one patch and dispersal performed by a single species. Then we explore the factors that govern synchrony between populations at the same or different trophic levels. In particular, we carefully examine the effects of perturbations depending on (1) which species have the strongest response to perturbations and (2) for which trophic level the strength of dispersal relative to demographic processes is highest. Finally, we try to disentangle the effects of several independent perturbations affecting different species. As a starting point, we consider a simple setting with Lotka-Volterra dynamics and stochastic external perturbations around an equilibrium. This allows us to partition the variability and correlations generated by multiple perturbations. Partitioning approaches provide a powerful way to disentangle the effects of different mechanisms and to assess their relative importance (Price 1970; Loreau and Hector 2001; Jaillard et al. 2018). It also allows us to use simple scenarios in which a single species is perturbed as building blocks to understand more complex systems with multiple perturbations. Thus, we

could assess the contribution of each species and their influence on other species to explain the synchrony or the asynchrony between the different populations.

Material and Methods

The Metacommunity Model

We extend the model developed by Barbier and Loreau (2019). They considered a food chain model with a simple metabolic parametrization, for which they described the biomass distribution and their responses to perturbations. Their model corresponds to the "intrapatch dynamics" part of equations (1a) and (1b), to which we graft a dispersal term to consider a metacommunity with two patches (fig. 1*A*):

$$\frac{dB_1}{dt} = B_1(g_1 - D_1B_1 - \alpha_{2,1}B_2) + \delta_1(B_1' - B_1), \tag{1a}$$

$$\frac{dB_i}{dt} = \underbrace{B_i(-r_i - D_iB_i + \varepsilon\alpha_{i,i-1}B_{i-1} - \alpha_{i+1,i}B_{i+1})}_{\text{intrapatch dynamics}} + \underbrace{\delta_i(B_i' - B_i)}_{\text{dispersal}}. \tag{1b}$$

The term B_i is the biomass of trophic level i in the patch of interest, B_i' its biomass in the other patch, ε is the biomass conversion efficiency, and $\alpha_{i,j}$ is the interaction strength between consumer i and prey j. Species i disperses between the two patches at rate δ_i. The density-independent net growth rate of primary producers g_i in equation (1a), the mortality rate of consumers r_i in equation (1b), and the density-dependent mortality rate D_i scale with species metabolic rates m_i, as biological rates are linked to energy expenditure (see sec. S1-2 of the supplemental PDF [available online]):

$$g_1 = m_1g, \quad r_i = m_ir, \quad D_i = m_iD. \tag{2}$$

To get a broad range of possible responses, we assume the predator-prey metabolic rate ratio m and the interaction strength to self-regulation ratio a to be constant. These ratios capture the relations between parameters and trophic levels. This enables us to consider contrasting situations while keeping the model as simple as possible:

$$m = \frac{m_{i+1}}{m_i}, \quad a = \frac{\alpha_{i,i-1}}{D_i}, \quad d_i = \frac{\delta_i}{D_i}. \tag{3}$$

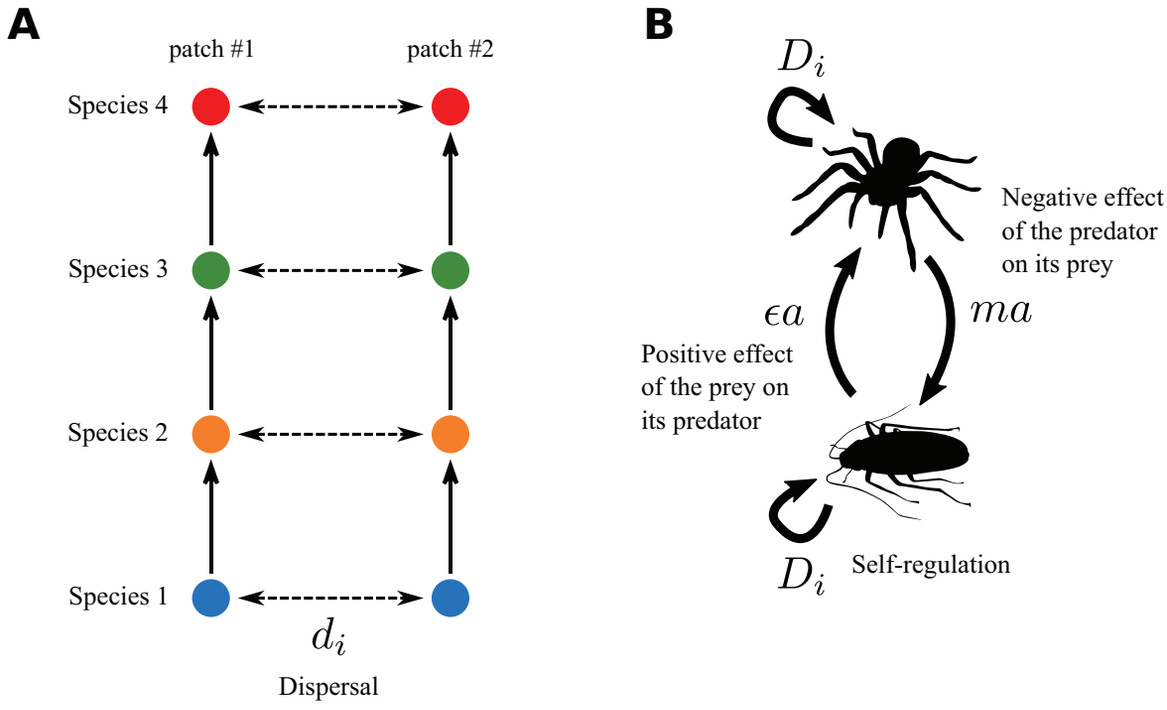

Figure 1: *A*, Metacommunity model with two patches, each containing a food chain with four trophic levels. Species disperse between the two patches at rate d_i. *B*, Predator-prey model with its synthetic parameters: εa is the positive effect of the prey on its predator, ma is the negative effect of the predator on its prey, and D_i is self-regulation.

Varying m leads to food chains where predators have faster or slower biomass dynamics than their prey, and varying a leads to food chains where interspecific interactions prevail or not compared with intraspecific interactions (fig. 1*B*). As all biological rates are rescaled by D_i, we also define d_i, the dispersal rate relative to self-regulation (referred as the "scaled dispersal rate" in the rest of the article), in order to keep the values of the dispersal rate relative to the other biological rates consistent across trophic levels. Finally, the timescale of the system is defined by setting the metabolic rate of the primary producer m_1 to unity. Thus, we can transform equations (1a) and (1b) into

$$\frac{1}{D}\frac{dB_1}{dt} = B_1\left(\frac{g}{D} - B_1 - maB_2\right) + d_1(B_1' - B_1), \tag{4a}$$

$$\frac{1}{m^{i-1}D}\frac{dB_i}{dt} = \underbrace{B_i\left(-\frac{r}{D} - B_i + \varepsilon aB_{i-1} - maB_{i+1}\right)}_{\text{intrapatch dynamics}} + \underbrace{d_i(B_i' - B_i)}_{\text{dispersal}}. \tag{4b}$$

Thus, εa and ma define the positive effect of the prey on its predator and the negative effect of the predator on its prey, respectively (fig. 1*B*). These two synthetic parameters define the overall behavior of the food chain and will be varied over the interval $[0.1, 10]$ (see table S1-2; tables S1-1 and S1-2 are available online) to consider a broad range of possible responses (for more details, see fig. 2*A* and Barbier and Loreau 2019). Parameter values are summarized in tables S1-1 and S1-2.

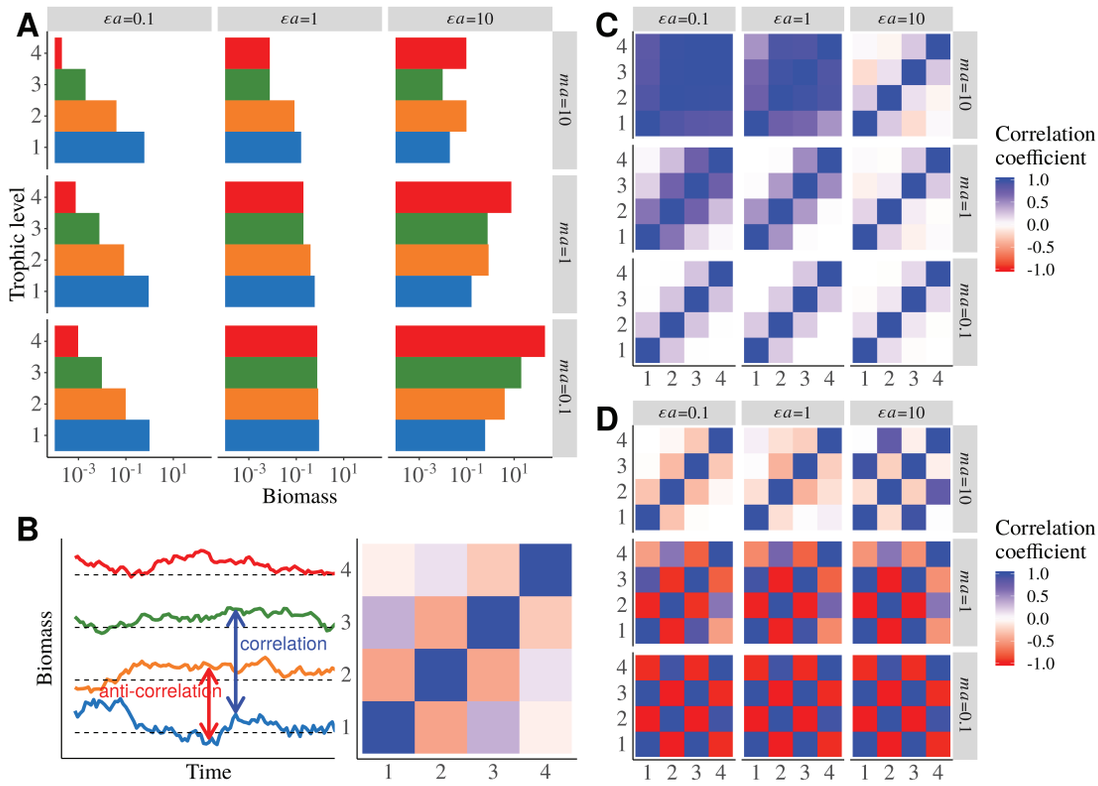

Figure 2: General description of an isolated food chain ($d_i = 0$, no dispersal) for nine combinations of the physiological and ecological parameters εa and ma that respectively describe the positive effect of biomass consumption and the negative effects of mortality due to predation (see Barbier and Loreau 2019). *A*, Biomass distribution among trophic levels. *B*, Correlation between species biomass dynamics. The correlations seen in the time series are represented by a correlation matrix where each element is the correlation coefficient between two species. Thus, the matrix is symmetric and the diagonal elements are equal to 1, as each species is perfectly autocorrelated. *C*, Correlation matrix within a food chain with a demographic stochastic perturbation applied to primary producers. *D*, Same correlation matrix with a demographic stochastic perturbation applied to top predators.

Stochastic Perturbations

To study the response of the metacommunity to perturbations, we apply stochastic perturbations. From equations (4a) and (4b) we get the following stochastic differential equation:

$$dB_i = \underbrace{f_i(B_1, \dots, B_S)\, dt}_{\text{deterministic}} + \underbrace{\sigma_i B_i^z dW_i}_{\text{perturbation}}. \quad (5)$$

The term $f_i(B_1, \dots, B_S)$ represents the deterministic part of the dynamics of species i biomass depending on the biomass of the S species present in the metacommunity (as described by eqq. [4a] and [4b]). Stochastic perturbations are defined by their standard deviation σ_i and dW_i, a white-noise term with mean 0 and variance 1. In addition, perturbations scale with each species biomass with an exponent z. We consider two types of perturbations (Haegeman and Loreau 2011; Arnoldi et al. 2019): demographic stochasticity (from birth-death processes) corresponds to $z = 0.5$, and environmental factors lead to $z = 1$ (see the demonstration in sec. S1-3 of the supplemental PDF and in Lande et al. 2003). Arnoldi et al. (2019) showed that when a species is perturbed, the ratio of its biomass variance to the perturbation variance increases with the species' biomass in the case of environmental perturbations, while it is independent of its biomass in the case of demographic perturbations. Therefore, we chose demographic perturbations in our analysis, as they enable us to perturb different species with the same relative intensity regardless of their abundance. This choice is made purely for modeling convenience. Although environmental perturbations may be more relevant from an ecological point of view, changing the perturbation exponent will alter only which trophic level is most affected (e.g., the most abundant, for environmental perturbations), not the rest of our analysis (see fig. S2-5; figs. S2-1–S2-5 are available online).

Response to Perturbations

We aim to determine the synchrony between populations at equilibrium when they receive small stochastic perturbations. Synchrony can be evaluated from the covariance between the temporal variations of different species and patches, which are encoded in the variance-covariance matrix C^*. Therefore, we linearize the system in the vicinity of equilibrium to get equation (6), where $X_i = B_i - B_i^*$ is the deviation from equilibrium (see secs. S1-4 and S1-6 of the supplemental PDF):

$$\frac{dX}{dt} = JX + TE. \quad (6)$$

The term J is the Jacobian matrix (see sec. S1-5 of the supplemental PDF), and T defines how the perturbations $E_i = \sigma_i dW_i$ apply to the system (scaling with species biomass).

Then we get the variance-covariance matrix C^* of species biomasses (variance-covariance matrix of X) from the variance-covariance matrix of perturbations V_E (variance-covariance matrix of E) by solving the Lyapunov equation (7) (Arnold 1974; Wang et al. 2015; Arnoldi et al. 2016; Shanafelt and Loreau 2018):

$$JC^* + C^*J^\top + TV_ET^\top = 0. \quad (7)$$

The expressions of V_E and T and the method to solve the Lyapunov equation are detailed in section S1-6 of the supplemental PDF. The variance-covariance matrix C^* can also be obtained through numerical simulations with the Euler-Maruyama method, which is detailed in section S1-7 of the supplemental PDF.

From the variance-covariance matrix C^* whose elements are w_{ij}, we can compute the correlation matrix R^* of the system whose elements ρ_{ij} are defined by

$$\rho_{ij} = \frac{w_{ij}}{\sqrt{w_{ii}w_{jj}}}. \quad (8)$$

Processes Controlling the Synchrony

We first explore the general response of the food chain model to perturbations affecting specific trophic levels (or when trophic levels are perturbed). Thus, we show how the perturbations propagate vertically through the food chain depending on various ecological conditions described by the synthetic parameters summarized in figure 1*B*. Then we study a simple case where only one species is perturbed and one species is able to disperse in order to identify the mechanisms leading to the asynchrony of the two populations of the same species. We finish with two more complex settings: one where all trophic levels are able to disperse at the same rate, and one where all trophic levels in the two patches are affected by independent perturbations.

In the first setting, we identify the factors controlling the relative importance of demographic and dispersal processes: dispersal processes tend to correlate (or anticorrelate) populations, while demographic process tend to decorrelate them. We define a metric M_1 that describes the relative weight of these two processes by taking the absolute values of the elements of equations (4a) and (4b) to assess the sheer intensity of local demographic processes and dispersal processes calculated with the equilibrium biomasses:

$$M_1 = \frac{|d_i B_i^{*\prime}| + |-d_i B_i^*|}{\begin{pmatrix} |\varepsilon a B_{i-1}^* B_i^*| + |d_i B_i^{*\prime}| + |-\frac{r}{D} B_i^*| \\ + |-B_i^{*2}| + |-maB_{i+1}^* B_i^*| + |-d_i B_i^*| \end{pmatrix}}. \quad (9)$$

In the second setting, we use the Lyapunov equation to partition the effect of each perturbation and to disentangle the contribution of each perturbation and each trophic level to the correlation pattern.

Results

General Responses of the Food Chain Model to Perturbations

We first describe the biomass distribution and the responses to perturbations of an isolated food chain (i.e., without considering spacial dynamics). We use a broad range of physiological and ecological parameters to describe all of the possible responses of the food chain model (fig. 2*A*). The term ma represents the strength of negative interactions (mortality due to predation), while εa represents the strength of positive interactions (biomass gain due to consumption; fig. 1*B*). As in Barbier and Loreau (2019), the food chain displays various biomass distributions in different regimes: bottom-heavy biomass pyramids (for $\varepsilon a = 0.1$), top-heavy biomass pyramids (for $\varepsilon a = 10$ and $ma = 0.1$), or alternating "cascade" patterns (for $\varepsilon a = 10$ and $ma = 10$).

In each case, we can capture the dynamical behavior of the food chain by considering the correlation matrix of the response of each species to perturbations applied to specific trophic levels (fig. 2*B*). Perturbing primary producers leads to bottom-up responses in which adjacent trophic levels are correlated (i.e., their biomasses respond in the same way; fig. 2*B*, 2*C*), while perturbing top predators leads to top-down responses in which adjacent trophic levels are anticorrelated (i.e., their biomasses respond in opposite ways; fig. 2*B*, 2*D*).

When all species receive independent stochastic demographic perturbations (fig. S2-1*A*), the correlation pattern is dominated by bottom-up effects for high values of ma ($ma = 10$, which corresponds to the strongest responses in fig. 2*C*) and is top down for low values of ma ($ma \leq 1$, which corresponds to the strongest responses in fig. 2*D*; see also fig. S2-1*C*).

Propagation of a Perturbation When One Species Disperses

Perturbations can propagate vertically within a food chain or horizontally between food chains. To understand how these two types of propagations shape the synchrony between patches, we first consider a simple case where only primary producers are perturbed in patch 1 (patch 2 being the unperturbed patch) and only top predators disperse (fig. 3*A*).

In patch 1, the perturbation has a bottom-up effect that correlates species (fig. 3*B*, label 1) as in figure 2*C*, where primary producers are also directly perturbed. While in patch 2, the perturbation has a top-down transmission (fig. 3*A*), leading to an anticorrelation of adjacent trophic levels (fig. 3*B*, label 2), which is similar to figure 2*D*, as the transmission of the perturbation by top predators is equivalent to a direct perturbations of top predators in patch 2. Then the different correlation patterns within each patch affect the synchrony between the two patches. First, the two populations of top predators are perfectly correlated, as they are directly coupled through dispersal (fig. 3*B*, label 3). Second, the populations of carnivores are anticorrelated because they are respectively correlated and anticorrelated to top predators in patches 1 and 2 (fig. 3*B*, label 4). Similarly, the correlation between each trophic level and top predators in each patch drives the correlation between the two populations at lower trophic levels.

For Whom Does Dispersal Matter?

Now all species disperse at the same rate d_i, but we still consider perturbations only affecting the primary producers in patch 1. Even if all scaled dispersal rates are equal, the relative importance of dispersal processes compared with intrapatch demography quantified by M_1 (see eq. [9]) differs between species. When scaled dispersal rates d_i increase, M_1 increases first for top predators, then for carnivores and so on until it increases for primary producers (fig. 4*E*). This is due to biomass distribution (fig. 2*A*), as dispersal scales linearly with biomass while intrapatch demography scales with squared biomass (self-regulation) or biomass products (predation; see eqq. [4a] and [4b] as well as fig. S2-1*E* in the supplemental PDF).

At low scaled dispersal rates (e.g., $d_i = 10^{-4}$), dispersal matters only for top predators (fig. 4*E*, label A), leading to a situation already described by figure 3. At intermediate scaled dispersal rates (e.g., $d_i = 10^{-2.6}$), dispersal also matters for carnivores (fig. 4*E*, label B). Thus, top predators and carnivores are correlated between patches, and we observe anticorrelations between adjacent trophic levels lower than 4 (fig. 4*B*). This time, this leads to the anticorrelation of subpopulations of herbivores (fig. 4*F*, label B), while they were correlated previously (fig. 3*B* and fig. 4*F*, label A). Therefore, each time dispersal starts to matter for another trophic level, the correlation pattern in patch 2 changes (fig. 4*A*–4*D*), leading to shifts between correlations

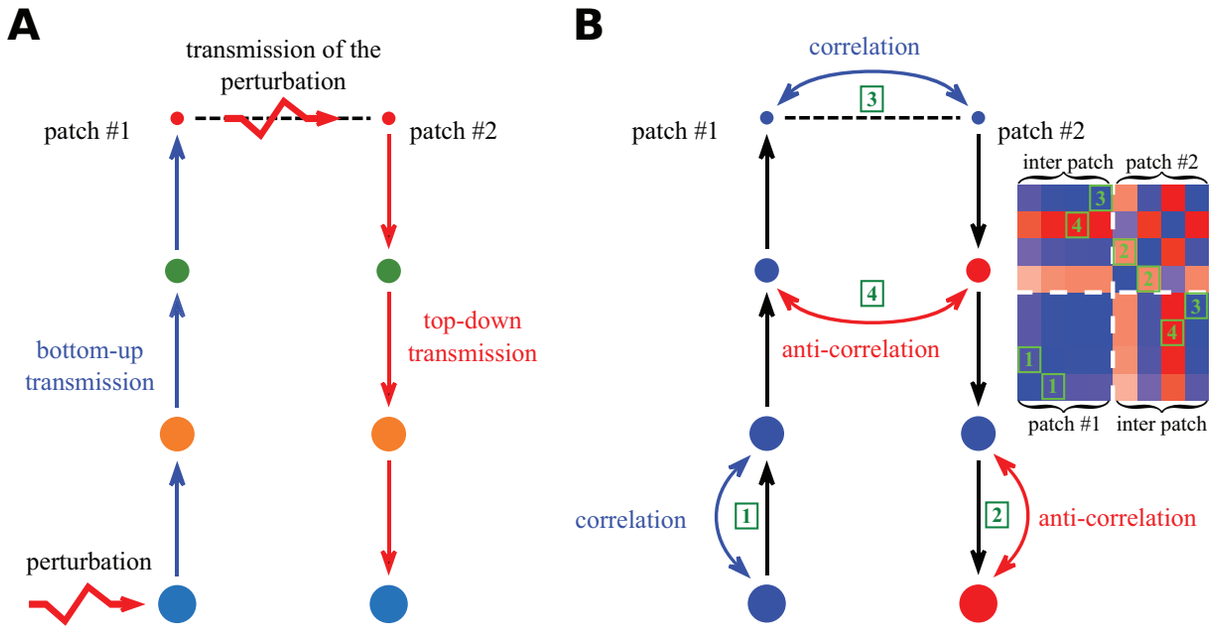

Figure 3: Transmission of perturbations between the two patches (primary producers perturbed in patch 1, $\varepsilon a = 0.1$, $ma = 10$, and only top predators disperse). Disk size represents species abundance. *A*, Only top predators are able to disperse, transmitting the perturbation between patches. They convert the bottom-up perturbation from patch 1 into a top-down perturbation in patch 2. *B*, The bottom-up transmission in patch 1 leads to correlations between adjacent trophic levels (label 1), while the top-down transmission leads to anticorrelations between adjacent trophic levels in patch 2 (label 2). Dispersal directly couples the two populations of top predators that act as one unique population; thus, they are completely correlated (label 3). The different correlation patterns within each patch lead to correlations or anticorrelations between populations of the same species in different patches depending on its distance from top predators (label 4).

and anticorrelations between the populations of lower trophic levels (fig. 4*F*).

Multiple Perturbation Partitioning

The case displayed in figure 4 was easy to handle, as only one perturbation was applied and we knew for which species dispersal mattered. Such a simple case can actually act as a building block to understanding correlation patterns produced by multiple perturbations. In fact, for R independent perturbations, the variance-covariance matrix C_S^* is equal to the sum of the variance-covariance matrices $C_{S,j}^*$ obtained when only one perturbation j is applied, $C_S^* = \sum_{j=1}^{R} C_{S,j}^*$ (see sec. S2-3-1 of the supplemental PDF). Then correlations between the populations of species i can be expressed as the sum of the correlations obtained when each perturbation j is applied alone weighted by the corresponding variance in the two patches:

$$\rho_i = \sum_{j=1}^{R} \rho_{i,j} M_{2_j} M_{3_j}. \tag{10}$$

The term R is the number of independent perturbations, ρ_i is the correlation coefficient between the two populations of species i, and $\rho_{i,j}$ is the same correlation coefficient in the case where only perturbation j is applied. The term M_{2_j} quantifies the variability generated locally by perturbation j that is effectively transmitted to the other patch (fig. 5*A*). If M_{2_j} is close to zero, the perturbation is poorly transmitted, and the two patches will probably be asynchronous. The term M_{3_j} weights each $\rho_{i,j}$ by the variability generated by perturbation j compared with the other perturbations (fig. 5*B*). If M_{3_j} is low, perturbation j would generate less variability than the other perturbations, and the associated correlation $\rho_{i,j}$ will not significantly contribute to the correlation ρ_i generated by all perturbations.

In the following, we present a simple case with two species in each patch receiving independent demographic stochastic perturbations and only primary producers are able to disperse (for an example with four species, see fig. S2-3). In figure 6, we illustrate step by step the decomposition of the correlation pattern generated by multiple perturbations (fig. 6*G*).

When only primary producers are perturbed in patch 1, both primary producers and herbivores are correlated because of the bottom-up transmission of the perturbation in both patches, as only primary producers disperse (fig. 6*A*). However, when only herbivores are perturbed, herbivores

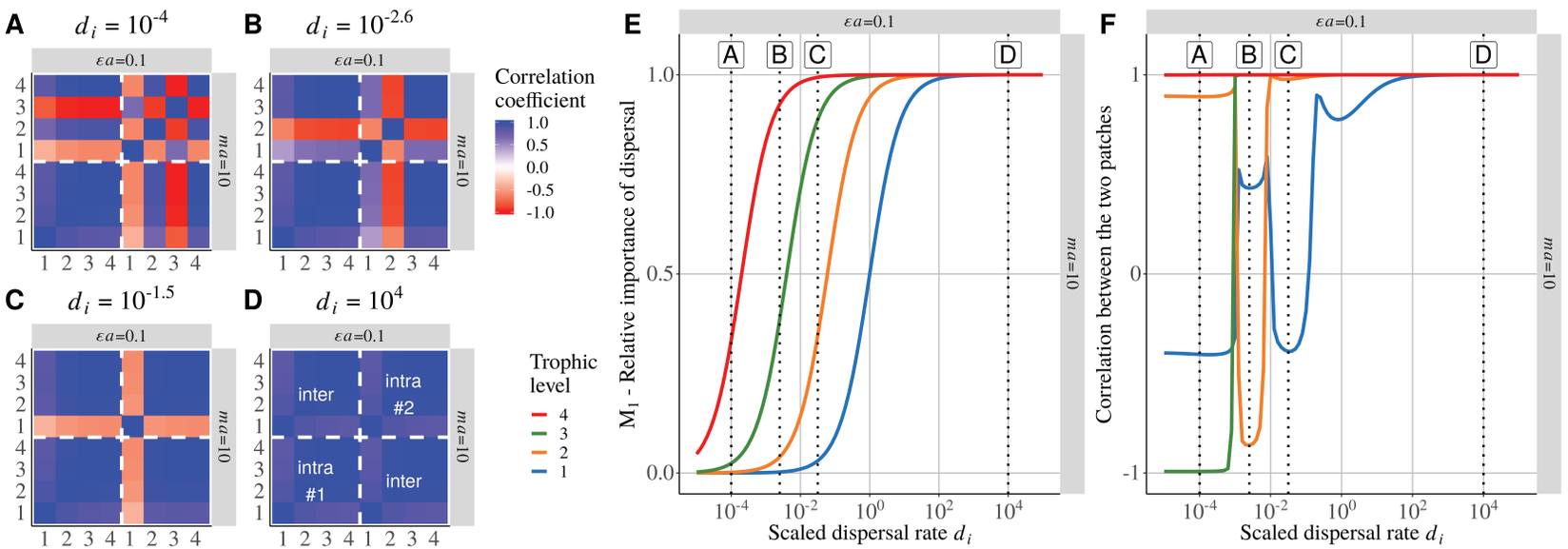

Figure 4: Correlation between populations of four species forming a food chain present in two connected patches ($\varepsilon a = 0.1$, $ma = 10$). Primary producers in patch 1 receive demographic perturbations, while patch 2 is not directly perturbed. *A–D* are correlation matrices between species within and between patches for four different scaled dispersal rates d_i. Diagonal blocks represent intrapatch species correlations, while the other blocks represent interpatch species correlations (see the labels in *D*). The bottom left block represents the perturbed patch (patch 1), while the top right block represents the unperturbed patch (patch 2; see fig. 3*B*). *E*, M_1, the ratio of dispersal processes to the sum demographic and dispersal processes (see eq. [9]) for each trophic level with increasing scaled dispersal rates. Labels A, B, C, and D respectively refer to the values of scaled dispersal rates used to plot the correlation matrices presented in *A*, *B*, *C*, and *D*. *F*, Correlation between populations of the same species from two patches for increasing scaled dispersal rates d_i (equal for all species). The represented correlations are equal to the diagonal elements of the off-diagonal blocks of the correlation matrix ("inter").

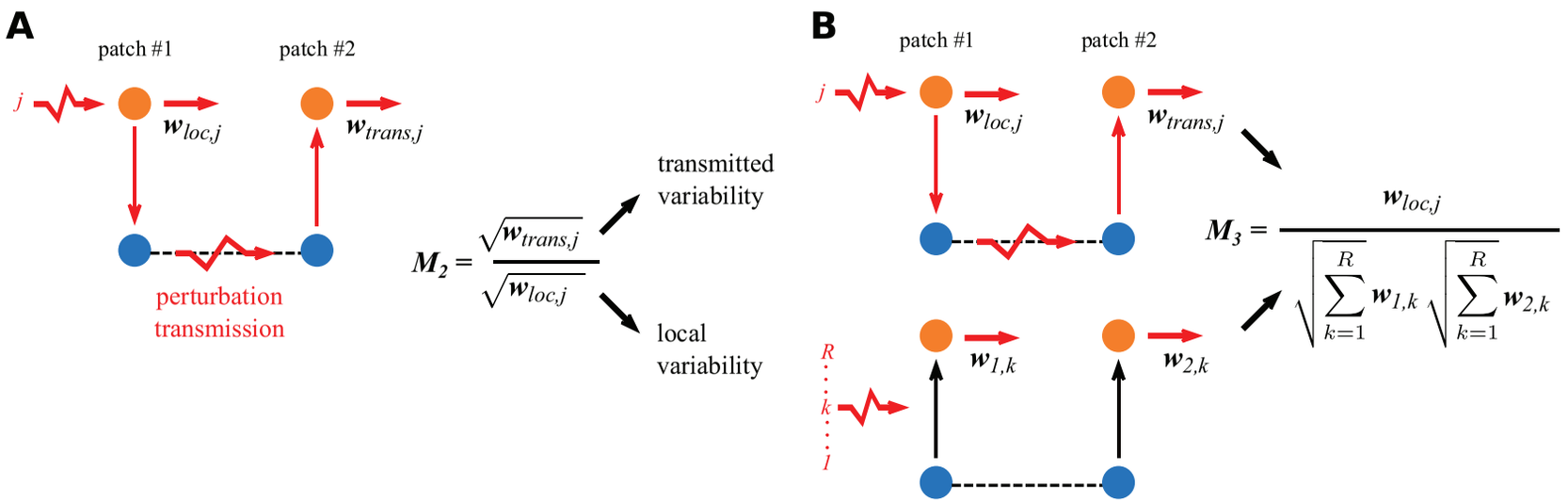

Figure 5: Metrics weighting the contribution of each perturbation to the correlation pattern generated by multiple perturbations. $w_{1,j}$ and $w_{2,j}$, which are elements of the matrix $C^*_{S,j}$, are the variance of species i in patches 1 and 2, respectively, when perturbation j is applied. We define $w_{\mathrm{loc},j}$ as the variability directly generated by the perturbation and $w_{\mathrm{trans},j}$ as the variability transmitted in the other patch. $w_{\mathrm{loc},j}$ and $w_{\mathrm{trans},j}$ are respectively equal to $w_{1,j}$ (or $w_{2,j}$) and $w_{2,j}$ (or $w_{1,j}$) when perturbation j is applied in patch 1 (or patch 2). *A*, M_{2_j} is the ratio of transmitted variability $w_{\mathrm{trans},j}$ to local variability $w_{\mathrm{loc},j}$. *B*, M_{3_j} weights the effect of each perturbation j by the variability it generates locally compared with the other perturbations.

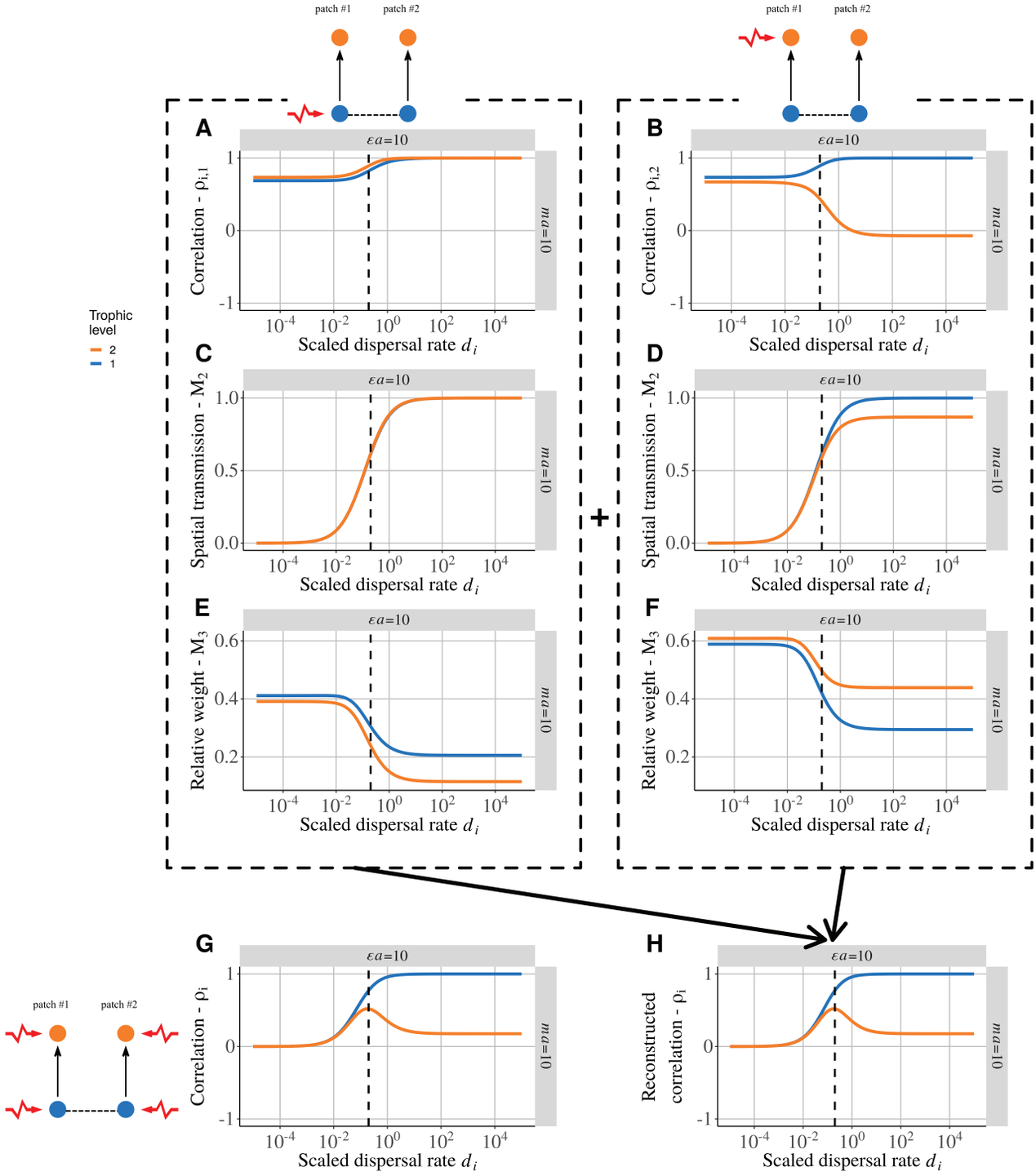

Figure 6: Detailed correlation pattern between two coupled primary producer-herbivore food chains for $\varepsilon a = 10$ and $ma = 10$ with increasing scaled dispersal rates d_i. Only primary producers are able to disperse. *A*, *B*, Correlation between patches when only primary producers (*A*) and herbivores (*B*) from patch 1 are perturbed. *C*, *D*, Relative importance of transmitted variability to local variability (M_2) when primary producers (*C*) and when herbivores (*D*) are perturbed in patch 1. *E*, *F*, Relative weight of the variance generated by each perturbation (M_3) when primary producers (*E*) and when herbivores (*F*) are perturbed in patch 1. *G*, Correlation between patches when independent demographic stochastic perturbations are applied to all species of each patch. *H*, Reconstructed correlation pattern obtained thanks to equation (10). $H = 2(A \times C \times E + B \times D \times F)$ by symmetry, as patches 1 and 2 receive similar independent perturbations.

become decorrelated, as scaled dispersal rates d_i increase (fig. 6*B*) because of the weak correlation between adjacent trophic levels for $\varepsilon a = 10$ and $ma = 10$ (see fig. 2*C*, 2*D*).

Our metric M_2 is equal to zero at low scaled dispersal rates d_i (fig. 6*C*, 6*D*), thus indicating that the perturbations in patch 1 are weakly transmitted in patch 2. At high scaled dispersal rates d_i, M_2 tends to 1, as species become perfectly correlated except for herbivores in figure 6*D*. In this case, as they are perturbed but do not disperse, the perturbation is attenuated during its transmission through primary producers.

In this example, our metric M_3 is higher for both primary producers and herbivores when the perturbation is applied to herbivores (fig. 6*F*) than when it is applied to primary producers (fig. 6*E*). This means that perturbations applied to herbivores generate most of the variability in the metacommunity, and the correlation pattern in figure 6*B* thus strongly contributes to the reconstructed correlation pattern gathering the effects of all perturbations (fig. 6*H*), following equation (10).

Now we have the response of all of the elements of equation (10), we can explain the correlation pattern seen in figure 6*H*. At low scaled dispersal rates d_i, perturbations are not transmitted ($M_2 = 0$), leaving the two patches independent and uncorrelated, while at high scaled dispersal rates d_i, the correlation pattern is similar to figure 6*B*, as herbivore perturbation generates most of the variability. In between, we have a humped-shaped relationship between herbivore population correlation and scaled dispersal rates d_i because when perturbations start to be transmitted (fig. 6*C*, 6*D*), herbivore populations are correlated (left of the dashed line; fig. 6*A*, 6*B*). Then the decrease in figure 6*B* leads to the decrease seen in figure 6*H*.

The reconstructed correlation pattern in figure 6*H* is identical to the correlation pattern obtained by perturbing directly each species in each patch (fig. 6*G*), thus demonstrating the validity of equation (10) (see fig. S2-4).

Discussion

Our metacommunity model aimed to understand how perturbations propagate vertically in patches and horizontally between patches to identify under which conditions species responses in different patches can be synchronous or asynchronous. First, we found that less abundant species are more affected by dispersal. Thus, even when all species disperse at the same scaled rate, the biomass distribution in a food chain determines for which species dispersal contributes the most to biomass dynamics. In addition, if the perturbed species does not disperse enough to synchronize its different populations, the perturbation can be transmitted by other species. In such a situation, we found that species responses in different patches can be asynchronous. Second, we found that the effects of multiple independent perturbations can be partitioned. This enabled us to use simple situations in which a single species is perturbed as building blocks to analyze more complex systems with multiple perturbations. Thus, we were able to identify which perturbations drove synchrony or asynchrony in this context and thus to explain their contribution using two simple metrics.

For Whom Does Dispersal Matter?

Knowing who disperses is crucial to understanding biomass dynamics in metacommunities (Koelle and Vandermeer 2005; Pedersen et al. 2016). However, even when dispersal is homogeneous among the various species (i.e., same scaled dispersal rates d_i for all species), increasing dispersal does not affect all species in the same way (fig. 7). In fact, abundant species are more affected by demographic processes such as self-regulation, which scales as the square of biomass, or trophic interactions, which scale as the product of predator and prey biomass (see eq. [9]). Thus, changes in scaled dispersal rates lead to top-down or bottom-up coupling between patches depending on biomass distribution.

Once we know for whom dispersal matters, the model can be simplified to a metacommunity where only a few species connect patches. With such a restricted dispersal, perturbing a species in one patch can lead to an opposite response in the other connected patch. In fact, perturbations affecting basal species have a bottom-up propagation (fig. 2*C*) and correlate all the species from the same food chain, while perturbations affecting top species have a top-down propagation and create trophic cascade correlation patterns (fig. 2*D*). Thus, if the perturbed species are not the dispersing species, both patches can display different correlation patterns, which can lead to anticorrelated responses of the different populations of the same species and hence to asynchrony between the different populations (figs. S2-1*E*, S2-2*A*, S2-2*B*). The correlation or anticorrelation of populations depends on the shortest trophic distance from the dispersing species, as suggested by Wollrab et al. (2012). Species at odd distance have correlated population fluctuations, while species at even distance have anticorrelated population fluctuations (fig. 3*A*).

The case where bottom-up perturbations are transmitted by top predators is related to the spillover process: a predator population thrives as a result of resource abundance in one patch and spills over to the other patches (Holt 1984). For instance, favorable environmental conditions in the Baltic main basin increase cod abundance (bottom-up control) that colonize the Gulf of Riga, leading to a trophic cascade in this locality (top-down response; Casini et al. 2012). More generally, predators cast a "shadow" that leads to trophic cascades around their source patch

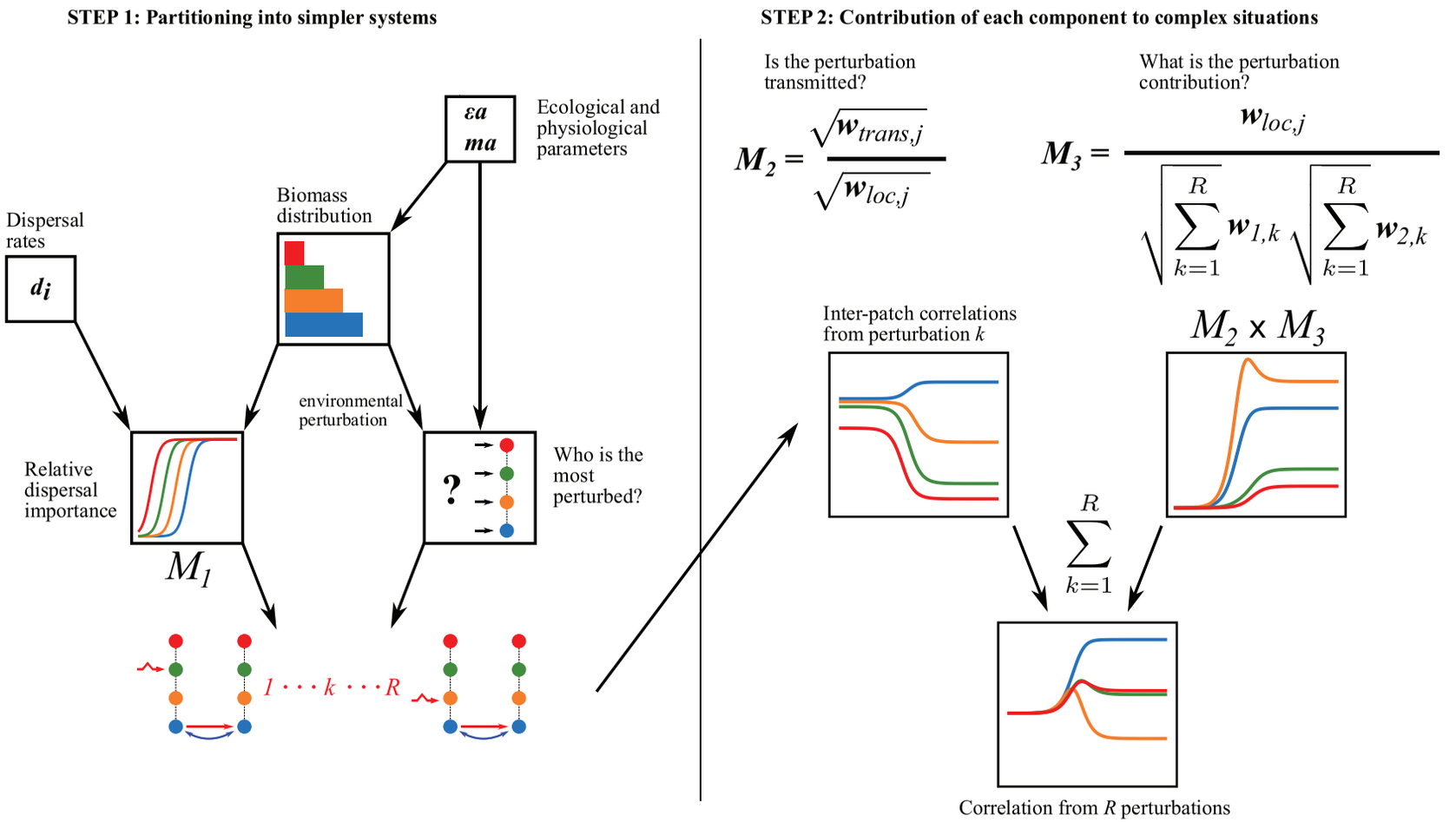

Figure 7: Sequential framework to understand the transmission of perturbations in metacommunities. Biomass distribution (driven by physiological and ecological parameters) is central, as less abundant species are more affected by dispersal (metric M_1) and are less affected by environmental perturbations. Knowing that, we can simplify the system into a metacommunity where only a few species disperse and are perturbed. The effects of each perturbation can then be partitioned to understand how much they contribute to the total correlation between patches. The contribution of each perturbation can be interpreted by two metrics: M_2, which quantifies how much of the generated variability is transmitted through dispersal, and M_3, which quantifies the how much variability is generated compared with other perturbations. Therefore, $M_2 \times M_3$ weights the correlation generated by each perturbation to reconstruct the correlation pattern obtained when multiple perturbations are applied.

(McCoy et al. 2009). For instance, dragonflies that prey on flying insects around ponds reduce pollination there (Knight et al. 2005). Such dynamics of predators between natural habitats and crop fields are central in pest biocontrol (Tscharntke et al. 2012).

The bottom-up coupling between patches does not seem to be mediated by primary producers, which often have a low mobility (sessile terrestrial plants or drifting phytoplankton), but rather by nonliving materials (Polis et al. 1997; Leroux and Loreau 2008). Marleau et al. (2010) and Gounand et al. (2014) found in their models with limit cycles that flows of nutrients lead to anticorrelations between species populations, while we found a succession of correlations and anticorrelations. This suggests that systems with limit cycles respond differently to bottom-up coupling than systems in the vicinity of an equilibrium that receive stochastic perturbations because of processes such as phase locking (Jansen 1999; Liebhold et al. 2004; Vasseur and Fox 2009). Abiotic resources can link very different food webs. For instance, mineral nutrients and dead organic matter link green and brown food webs (Wolkovich et al. 2014; Buchkowski et al. 2019), but additional mechanisms, such as different food chain length, omnivory, or stoichiometric constraints (Attayde and Ripa 2008; Zou et al. 2016), make a direct comparison difficult. Nevertheless, our model gives basic insights into how a simple bottom-up coupling affects the dynamics of connected food chains and should improve our understanding of the additional effects brought by mechanisms such as different food chain length or stoichiometric constraints.

While top predator dispersal or basal resource diffusion have been extensively studied, the consequences of intermediate trophic level dispersal remain poorly understood. Our results show that the dispersal of intermediate trophic levels can dramatically change the correlation between populations of nondispersing species. Pedersen et al. (2016) found that herbivores with a lower dispersal rate than primary producers or carnivores stabilize metacommunity dynamics (by having equilibriums or asynchronous limit cycles).

Most of the studies of coupled food webs considered systems displaying limit cycles (McCann et al. 1998; Post et al. 2000; Koelle and Vandermeer 2005) and largely ignored stochastic perturbations (McCann et al. 2005; Vasseur and Fox 2007). Our results suggest that dispersal patterns that lead to more asynchrony depend on which species is perturbed. If the most perturbed species is also the most affected by dispersal, it transmits the perturbation to all patches and synchronizes them, thus reducing the stability of the system. Otherwise, asynchrony between patches can be promoted. Thus, the stabilizing or destabilizing effect of dispersal patterns is not absolute and depends on perturbations.

In addition, perturbations can target specific species (e.g., harvesting, disease) or affect all of the species in different ways. For instance, Arnoldi et al. (2019) showed that environmental perturbations ($z = 1$) mostly affect abundant species (figs. 7, S2-1*B*, S2-2*D*, S2-5). Therefore, considering the biomass distribution is critical to fully understanding the responses of coupled food chains to dispersal and perturbations.

Multiple Perturbation Partitioning

Complex correlation patterns produced by multiple independent perturbations on different species in different patches can be easily partitioned into a sum of correlation patterns produced by a single perturbation (fig. 7). Such a partitioning is permitted by two characteristics of our model. First, the system is linearized. Thus, the temporal variations of each species in the vicinity of the equilibrium are the sum of the variations due to each interacting species. Second, the partitioning of the correlation pattern is permitted by the independence of the various perturbations. In fact, we can decompose the variance-covariance matrix of perturbation V_E into a sum of matrices V_{Ej} corresponding to the perturbation of a single species in a single patch (see eq. [21] in sec. S2-3-1 of the supplemental PDF). If some perturbations are correlated, we can still decompose the matrix V_E into a sum of independent blocks of correlated perturbations. The contribution of each perturbation in an assemblage of many independent perturbations can thus be easily understood, as the product of the correlations between populations from the two patches is weighted by the variability generated in each patch (fig. 7).

Such a detailed partition of the contribution of each element of the system is not possible in systems displaying nonlinear dynamics. For instance, Koelle and Vandermeer (2005) tested the effects of primary producer and top predator dispersal on population synchrony. They found that these two types of dispersal led to either asynchrony or synchrony between the populations of the other trophic levels, but they were unable to go deeper in their interpretation. Their results are similar to our case where a perturbation is applied to top predators only and primary producers disperse (fig. S2-2*B*). Thus, the top predator-prey interaction must generate most of the variability in their system with limit cycles and may be equivalent to a perturbation of top predators in our linear system. Therefore, our model with linear dynamics could give clues to understanding the response of models with nonlinear dynamics. Future investigations considering stochastic perturbations in models with type II functional responses are required to go deeper in the comparison between systems with linear or nonlinear dynamics.

Independence between perturbations is also a key feature of our study, as we explained earlier. Correlations between perturbations is expected to change the observed dynamics (Ripa and Ives 2003; Vasseur and Fox 2007). Leroux and Loreau (2012) considered reciprocal pulsed subsidies within a metacommunity model and demonstrated that the time delay between perturbations in each patch could reinforce or dampen the resulting oscillations. This suggests that the correlation pattern observed in our model when species from both patches are perturbed should be modified if perturbations are more or less correlated.

Conclusion

Our model demonstrates that asynchrony between populations in trophic metacommunities is promoted when the species the most affected by dispersal is not directly perturbed. The effect of dispersal on biomass dynamics compared with local demographic processes depends on the biomass distribution in food chains even if all species disperse at the same scaled rate. Thus, our simple model can serve as a good null model to test mechanisms involved in dispersal. Our model must be considered as a null model in general as it relies on strong assumptions (e.g., m constant across the food chain) to build a simple model to derive broad conclusions (Barbier and Loreau 2019). The results of future studies considering more realistic situations will surely deviate from our model, but our conclusions should still be useful, as each predator-prey couple will correspond to one set of parameters used in our figures.

Dispersal can be seen as a mechanism of optimal foraging where predators follow their prey in the patch where they are the most abundant. Dispersal also enables prey to escape their predators by migrating into a "refuge" patch where they are less abundant. This can be represented by density-dependent dispersal rates, which have a strong impact on dynamics (Hauzy et al. 2010; Liu et al. 2016). However, density-dependent dispersal changes the relative importance of dispersal and local demography, as dispersal then scales with biomass similarly to self-regulation or predation, thus changing the interplay between dispersal and biomass distribution. Therefore, future studies should consider biomass distribution among species to properly assess the effects of dispersal on food chain dynamics.

When multiple perturbations are applied, the effects of each perturbation and each species can be partitioned in our model. Thus, future studies considering heterogeneity between patches would be able to isolate the contribution of the difference of parameters to food chain dynamics. For instance, Rooney et al. (2006) considered two food chains with different attack rates coupled by a mobile top predator. In this case, perturbation partitioning would enable us to deeply understand how such differences between food chains may dampen perturbation transmission or promote asynchrony.

Thus, our approach appears to be a promising tool to better understand the effects of many mechanisms that promote stability or asynchrony in coupled food chains or trophic metacommunities.

Acknowledgments

We thank Charlotte T. Lee and two anonymous reviewers for their constructive comments. This work was supported by the TULIP Laboratory of Excellence (ANR-10-LABX-41) and by a BIOSTASES Advanced Grant, funded by the European Research Council under the European Union's Horizon 2020 research and innovation program (666971).

Statement of Authorship

Conceptualization: P.Q., M.B., M.L. Funding acquisition: M.L. Model analysis: P.Q., M.B., M.L. Coding simulation: P.Q. Supervision: M.L. Original draft writing: P.Q. Review and editing: M.B., M.L.

Data and Code Availability

The C++ code for the simulations and the R code for the figures are available on Zenodo (https://doi.org/10.5281/zenodo.3613500).

Literature Cited

Abbott, K. C. 2011. A dispersal-induced paradox: synchrony and stability in stochastic metapopulations. Ecology Letters 14:1158–1169.

Amarasekare, P. 2008. Spatial dynamics of foodwebs. Annual Review of Ecology, Evolution, and Systematics 39:479–500.

Arnold, L. 1974. Stochastic differential equations: theory and applications. Wiley, New York.

Arnoldi, J.-F., M. Loreau, and B. Haegeman. 2016. Resilience, reactivity and variability: a mathematical comparison of ecological stability measures. Journal of Theoretical Biology 389:47–59.

———. 2019. The inherent multidimensionality of temporal variability: how common and rare species shape stability patterns. Ecology Letters 22:1557–1567.

Attayde, J. L., and J. Ripa. 2008. The coupling between grazing and detritus food chains and the strength of trophic cascades across a gradient of nutrient enrichment. Ecosystems 11:980–990.

Barbier, M., and M. Loreau. 2019. Pyramids and cascades: a synthesis of food chain functioning and stability. Ecology Letters 22:405–419.

Blasius, B., A. Huppert, and L. Stone. 1999. Complex dynamics and phase synchronization in spatially extended ecological systems. Nature 399:354–359.

Buchkowski, R. W., O. J. Schmitz, and M. A. Bradford. 2019. Nitrogen recycling in coupled green and brown food webs: weak effects of herbivory and detritivory when nitrogen passes through soil. Journal of Ecology 107:963–976.

Casini, M., T. Blenckner, C. Mollmann, A. Gardmark, M. Lindegren, M. Llope, G. Kornilovs, M. Plikshs, and N. C. Stenseth. 2012. Predator transitory spillover induces trophic cascades in ecological sinks. Proceedings of the National Academy of Sciences of the USA 109:8185–8189.

Díaz, S., J. Settele, E. Brondizio, H. T. Ngo, M. Guèze, J. Agard, A. Arneth, et al. 2019. Summary for policymakers of the global assessment report on biodiversity and ecosystem services of the Intergovernmental Science-Policy Platform on Biodiversity and Ecosystem Services. IPBES, Bonn.

García-Callejas, D., R. Molowny-Horas, M. B. Araújo, and D. Gravel. 2019. Spatial trophic cascades in communities connected by dispersal and foraging. Ecology 100:e02820.

Gounand, I., N. Mouquet, E. Canard, F. Guichard, C. Hauzy, and D. Gravel. 2014. The paradox of enrichment in metaecosystems. American Naturalist 184:752–763.

Haddad, N. M., L. A. Brudvig, J. Clobert, K. F. Davies, A. Gonzalez, R. D. Holt, T. E. Lovejoy, et al. 2015. Habitat fragmentation and its lasting impact on Earth's ecosystems. Science Advances 1: e1500052.

Haegeman, B., and M. Loreau. 2011. A mathematical synthesis of niche and neutral theories in community ecology. Journal of Theoretical Biology 269:150–165.

Hauzy, C., M. Gauduchon, F. D. Hulot, and M. Loreau. 2010. Density-dependent dispersal and relative dispersal affect the stability of predator-prey metacommunities. Journal of Theoretical Biology 266:458–469.

Holt, R. D. 1984. Spatial heterogeneity, indirect interactions, and the coexistence of prey species. American Naturalist 124:377–406.

Jaillard, B., C. Richon, P. Deleporte, M. Loreau, and C. Violle. 2018. An a posteriori species clustering for quantifying the effects of species interactions on ecosystem functioning. Methods in Ecology and Evolution 9:704–715.

Jansen, V. A. A. 1999. Phase locking: another cause of synchronicity in predator-prey systems. Trends in Ecology and Evolution 14:278–279.

Knight, T. M., M. W. McCoy, J. M. Chase, K. A. McCoy, and R. D. Holt. 2005. Trophic cascades across ecosystems. Nature 437:880–883.

Koelle, K., and J. Vandermeer. 2005. Dispersal-induced desynchronization: from metapopulations to metacommunities. Ecology Letters 8:167–175.

Lande, R., S. Engen, and B.-E. Sæther. 2003. Stochastic population dynamics in ecology and conservation. Oxford University Press, Oxford.

Leibold, M. A., and J. M. Chase. 2017. Metacommunity ecology. Vol. 59. Princeton University Press, Princeton, NJ.

Leibold, M. A., M. Holyoak, N. Mouquet, P. Amarasekare, J. M. Chase, M. F. Hoopes, R. D. Holt, et al. 2004. The metacommunity concept: a framework for multi-scale community ecology. Ecology Letters 7:601–613.

Leroux, S. J., and M. Loreau. 2008. Subsidy hypothesis and strength of trophic cascades across ecosystems. Ecology Letters 11:1147–1156.

———. 2012. Dynamics of reciprocal pulsed subsidies in local and meta-ecosystems. Ecosystems 15:48–59.

Liebhold, A., W. D. Koenig, and O. N. Bjørnstad. 2004. Spatial synchrony in population dynamics. Annual Review of Ecology, Evolution, and Systematics 35:467–490.

Liu, Z., F. Zhang, and C. Hui. 2016. Density-dependent dispersal complicates spatial synchrony in tri-trophic food chains. Population Ecology 58:223–230.

Loreau, M., and A. Hector. 2001. Partitioning selection and complementarity in biodiversity experiments. Nature 412:72–76.

Marleau, J. N., F. Guichard, F. Mallard, and M. Loreau. 2010. Nutrient flows between ecosystems can destabilize simple food chains. Journal of Theoretical Biology 266:162–174.

McCann, K., A. Hastings, and G. R. Huxel. 1998. Weak trophic interactions and the balance of nature. Nature 395:794–798.

McCann, K. S., J. B. Rasmussen, and J. Umbanhowar. 2005. The dynamics of spatially coupled food webs. Ecology Letters 8:513–523.

McCoy, M. W., M. Barfield, and R. D. Holt. 2009. Predator shadows: complex life histories as generators of spatially patterned indirect interactions across ecosystems. Oikos 118:87–100.

Pedersen, E. J., J. N. Marleau, M. Granados, H. V. Moeller, and F. Guichard. 2016. Nonhierarchical dispersal promotes stability and resilience in a tritrophic metacommunity. American Naturalist 187:E116–E128.

Polis, G. A., W. B. Anderson, and R. D. Holt. 1997. Toward an integration of landscape and food web ecology: the dynamics of spatially subsidized food webs. Annual Review of Ecology and Systematics 28:289–316.

Post, D. M., M. E. Conners, and D. S. Goldberg. 2000. Prey preference by a top-predator and the stability of linked food chains. Ecology 81:8–14.

Price, G. R. 1970. Selection and covariance. Nature 227:520–521.

Purvis, A., J. L. Gittleman, G. Cowlishaw, and G. M. Mace. 2000. Predicting extinction risk in declining species. Proceedings of the Royal Society of London B 267:1947–1952.

Ripa, J., and A. R. Ives. 2003. Food web dynamics in correlated and autocorrelated environments. Theoretical Population Biology 64:369–384.

Rooney, N., K. McCann, G. Gellner, and J. C. Moore. 2006. Structural asymmetry and the stability of diverse food webs. Nature 442:265–269.

Rooney, N., K. S. McCann, and J. C. Moore. 2008. A landscape theory for food web architecture. Ecology Letters 11:867–881.

Shanafelt, D. W., and M. Loreau. 2018. Stability trophic cascades in food chains. Royal Society Open Science 5:180995.

Tscharntke, T., J. M. Tylianakis, T. A. Rand, R. K. Didham, L. Fahrig, P. Batáry, J. Bengtsson, et al. 2012. Landscape moderation of biodiversity patterns and processes—eight hypotheses. Biological Reviews 87:661–685.

Vadeboncoeur, Y., K. S. McCann, M. J. V. Zanden, and J. B. Rasmussen. 2005. Effects of multi-chain omnivory on the strength of trophic control in lakes. Ecosystems 8:682–693.

Vander Zanden, M. J., and Y. Vadeboncoeur. 2002. Fishes as integrators of benthic and pelagic food webs in lakes. Ecology 83:2152–2161.

Vasseur, D. A., and J. W. Fox. 2007. Environmental fluctuations can stabilize food web dynamics by increasing synchrony. Ecology Letters 10:1066–1074.

———. 2009. Phase-locking and environmental fluctuations generate synchrony in a predator-prey community. Nature 460:1007–1010.

Wang, S., B. Haegeman, and M. Loreau. 2015. Dispersal and metapopulation stability. PeerJ 3:e1295.

Ward, C. L., K. S. McCann, and N. Rooney. 2015. HSS revisited: multi-channel processes mediate trophic control across a productivity gradient. Ecology Letters 18:1190–1197.

Wolkovich, E. M., S. Allesina, K. L. Cottingham, J. C. Moore, S. A. Sandin, and C. de Mazancourt. 2014. Linking the green and brown worlds: the prevalence and effect of multi-channel feeding in food webs. Ecology 95:3376–3386.

Wollrab, S., S. Diehl, and A. M. De Roos. 2012. Simple rules describe bottom-up and top-down control in food webs with alternative energy pathways. Ecology Letters 15:935–946.

Zelnik, Y. R., J.-F. Arnoldi, and M. Loreau. 2019. The three regimes of spatial recovery. Ecology 100:e02586.

Zou, K., E. Thébault, G. Lacroix, and S. Barot. 2016. Interactions between the green and brown food web determine ecosystem functioning. Functional Ecology 30:1454–1465.

Associate Editor: Charlotte T. Lee
Editor: Daniel I. Bolnick

"The chapters on the fishers, on Labrador, those on the agricultural and mineral resources, etc., are all to the purpose. The best game animal is the caribou, which still in vast herds traverses the island in periodical migrations from north to south; the moose is still common, and there is good salmon fishing." Figured: "On the Barrens. The Caribou, Buck and Doe." From the review of Hatton and Harvey's *Newfoundland* (*The American Naturalist,* 1884, 18:41–45).